

MIT Open Access Articles

Luminescence of III-IV-V thin film alloys grown by metalorganic chemical vapor deposition

The MIT Faculty has made this article openly available. **Please share** how this access benefits you. Your story matters.

Citation: Jia, Roger, et al. "Luminescence of III-IV-V Thin Film Alloys Grown by Metalorganic Chemical Vapor Deposition." *Journal of Applied Physics*, vol. 123, no. 17, May 2018, p. 175101. © 2018 Authors

As Published: <http://dx.doi.org/10.1063/1.5016443>

Publisher: AIP Publishing

Persistent URL: <https://hdl.handle.net/1721.1/121247>

Version: Final published version: final published article, as it appeared in a journal, conference proceedings, or other formally published context

Terms of use: Creative Commons Attribution 4.0 International license



Luminescence of III-IV-V thin film alloys grown by metalorganic chemical vapor deposition ^{EP}

Cite as: J. Appl. Phys. **123**, 175101 (2018); <https://doi.org/10.1063/1.5016443>

Submitted: 19 November 2017 . Accepted: 18 April 2018 . Published Online: 03 May 2018

Roger Jia, Tony Zhu, Vladimir ^{Bu}lović, and Eugene A. Fitzgerald ^{id}

COLLECTIONS

^{EP} This paper was selected as an Editor's Pick



View Online



Export Citation



CrossMark

ARTICLES YOU MAY BE INTERESTED IN

[Electroluminescent refrigeration by ultra-efficient GaAs light-emitting diodes](#)

Journal of Applied Physics **123**, 173104 (2018); <https://doi.org/10.1063/1.5019764>

[Integrating AlInN interlayers into InGaN/GaN multiple quantum wells for enhanced green emission](#)

Applied Physics Letters **112**, 201106 (2018); <https://doi.org/10.1063/1.5028257>

[Epitaxial growth of high quality InP on Si substrates: The role of InAs/InP quantum dots as effective dislocation filters](#)

Journal of Applied Physics **123**, 193104 (2018); <https://doi.org/10.1063/1.5029255>

Ultra High Performance SDD Detectors



See all our XRF Solutions

Luminescence of III-IV-V thin film alloys grown by metalorganic chemical vapor deposition

Roger Jia,¹ Tony Zhu,² Vladimir Bulović,² and Eugene A. Fitzgerald¹

¹Department of Materials Science and Engineering, Massachusetts Institute of Technology, Cambridge, Massachusetts 02139, USA

²Department of Electrical Engineering and Computer Science, Massachusetts Institute of Technology, Cambridge, Massachusetts 02139, USA

(Received 19 November 2017; accepted 18 April 2018; published online 3 May 2018)

III-IV-V heterovalent alloys have the potential to satisfy the need for infrared bandgap materials that also have lattice constants near GaAs. In this work, significant room temperature photoluminescence is reported for the first time in high quality III-IV-V alloys grown by metalorganic chemical vapor deposition. Pronounced phase separation, a characteristic suspected to quench luminescence in the alloys in the past, was successfully inhibited by a modified growth process. Small scale composition fluctuations were observed in the alloys; higher growth temperatures resulted in fluctuations with a striated morphology, while lower growth temperatures resulted in fluctuations with a speckled morphology. The composition fluctuations cause bandgap narrowing in the alloys—measurements of various compositions of $(\text{GaAs})_{1-x}(\text{Ge}_2)_x$ alloys reveal a maximum energy transition of 0.8 eV under 20% Ge composition rather than a continuously increasing transition with the decreasing Ge composition. Additionally, luminescence intensity decreased with the decreasing Ge composition. The alloys appear to act as a Ge-like solid penetrating a GaAs lattice, resulting in optical properties similar to those of Ge but with a direct-bandgap nature; a decrease in the Ge composition corresponds to a reduction in the light-emitting Ge-like material within the lattice. An energy transition larger than 0.8 eV was obtained through the addition of silicon to the $(\text{GaAs})_{1-x}(\text{Ge}_2)_x$ alloy. The results indicate significant promise for III-IV-V alloys as potential materials for small bandgap optical devices with previously unachievable lattice constants. © 2018 Author(s). All article content, except where otherwise noted, is licensed under a Creative Commons Attribution (CC BY) license (<http://creativecommons.org/licenses/by/4.0/>). <https://doi.org/10.1063/1.5016443>

INTRODUCTION

There is significant interest in finding infrared direct bandgap materials close to the GaAs lattice constant for photovoltaic and photonic applications. A direct bandgap of 1 eV, for example, is highly desired for multi-junction photovoltaic cells fabricated on GaAs substrates. Currently, most research on 1 eV bandgap materials has focused on alloys lattice-matched to GaAs by using complex III-V materials such as InGaAsSbN or attempted to work with lattice mismatched $\text{In}_{0.3}\text{Ga}_{0.7}\text{As}$ and employed a graded composition buffer layer.^{1–3} Both approaches pose numerous epitaxial challenges to ensure high quality materials, especially when attempting to integrate on smaller lattice constant materials such as Si or GaAs. Additionally, even smaller direct bandgaps on GaAs are interesting for mid- and long-wave optical detection applications. Typically, InAs- and InSb-based materials are used to create these small bandgaps, but the large lattice mismatch to GaAs forces these narrow bandgap materials to be formed on expensive, small substrates such as InP, InAs, and GaSb. Small direct bandgaps in materials with a smaller lattice constant would allow these more advanced IR detectors to be ported to large, inexpensive substrates such as GaAs or Ge.

Metastable $(\text{GaAs})_{1-x}(\text{Ge}_2)_x$ alloys grown by ion-beam sputtering have been studied in the past—absorption

spectroscopy indicates that the alloys have direct bandgaps ranging from 0.6 eV to 1.4 eV depending on the composition.^{4,5} These alloys are lattice matched to GaAs and thus could potentially be ideal materials for the applications mentioned above. However, no luminescence results were reported for those alloys. A later study using metalorganic chemical vapor deposition (MOCVD) produced $(\text{GaAs})_{1-x}(\text{Ge}_2)_x$ structures with pronounced phase separation⁶ that exhibited photoluminescence (PL) signals only at extremely low (5 K) temperatures.⁷ In this work, we report the MOCVD growth of III-IV-V alloys, including $(\text{GaAs})_{1-x}(\text{Ge}_2)_x$, with significantly different morphologies from those of the previous study and which demonstrate room temperature photoluminescence.

EXPERIMENT

III-IV-V alloy structures were grown on semi-insulating (001) GaAs substrates in a Thomas Swan/Aixtron close-coupled showerhead MOCVD reactor by codeposition of the relevant precursors (TMGa, TMIIn, AsH₃, SiH₄, and GeH₄). In all samples, a nominal 40 nm GaAs homoepitaxial layer was first grown on the substrates, followed by a 20 s N₂ ambient anneal prior to deposition of the alloy film. Growth temperature was varied between 575 °C and 700 °C depending on the specific sample. The system pressure during

growth was 250 Torr for all samples. A sample consisting of a nominal 100 nm thick $(\text{GaAs})_{0.77}(\text{Ge}_2)_{0.23}$ alloy film followed by 200 nm of GaAs was also grown to observe the quality of films deposited on top of an alloy.

The morphologies of the samples were analyzed by cross-sectional transmission electron microscopy (XTEM). Compositions were estimated using energy-dispersive X-ray spectroscopy (EDX). Room temperature photoluminescence (PL) was conducted using a 514.5 nm emission continuous-wave argon ion laser operating at an output power of 150 mW. The detectors used include an InGaAs detector with good responsivity between 1000 and 1650 nm and a strained InGaAs detector with a good responsivity between 1500 and 2550 nm. Low temperature (77 K) PL was conducted using a micro-photoluminescence setup with a 1060 nm emission continuous-wave diode laser at an output power of 90 mW. The detector used was an IR spectrometer with an InGaAs photodiode with a good responsivity between 1300 and 2050 nm.

RESULTS AND DISCUSSION

Alloy morphologies

The structure of several $(\text{GaAs})_{1-x}(\text{Ge}_2)_x$ alloy samples is shown in Fig. 1. All structures demonstrate single-crystal diffraction patterns in the TEM, and the varying contrast in the films in Fig. 1 arises from slight composition changes locally. TEM is very sensitive to strain arising from such

composition fluctuations when imaged in a proper two-beam condition.

Generally, we observe two types of morphologies—striations, similar to that seen in Fig. 1(a), or speckled, similar to that seen in Figs. 1(b) and 1(c). Striated morphologies have been observed in many ternary and quaternary III-V alloys that are known to exhibit short-length-scale phase separation under the appropriate conditions.^{8–12} By using a non-equilibrium technique such as MOCVD to grow the material, the low bulk diffusivities result in surface-driven phase instability. Striations are observed due to the composition variation in the initial deposited material, which then bias the incorporation of subsequently deposited atoms. The striations seen in our $(\text{GaAs})_{0.71}(\text{Ge}_2)_{0.29}$ alloy [Fig. 1(a)] are likely due to a similar mechanism. In this case, incorporation is biased by the preference of Ge to bond to Ge and GaAs to GaAs. Thus, relatively GaAs-rich regions will have GaAs-rich overgrowth, while relatively Ge-rich regions will have Ge-rich overgrowth, ultimately resulting in a striated morphology. The $(\text{GaAs})_{1-x}(\text{Ge}_2)_x$ alloys with speckled morphologies [Figs. 1(b) and 1(c)] clearly do not exhibit the growth mechanism described above. The likely explanation is the reduced adatom surface mobility as a result of the lower growth temperatures compared to the sample in Fig. 1(a). Reduced surface mobility kinetically limits the surface phase separation process, preventing the formation of striations. Instead, we observed a morphology similar to the early stage spinodal decomposition.

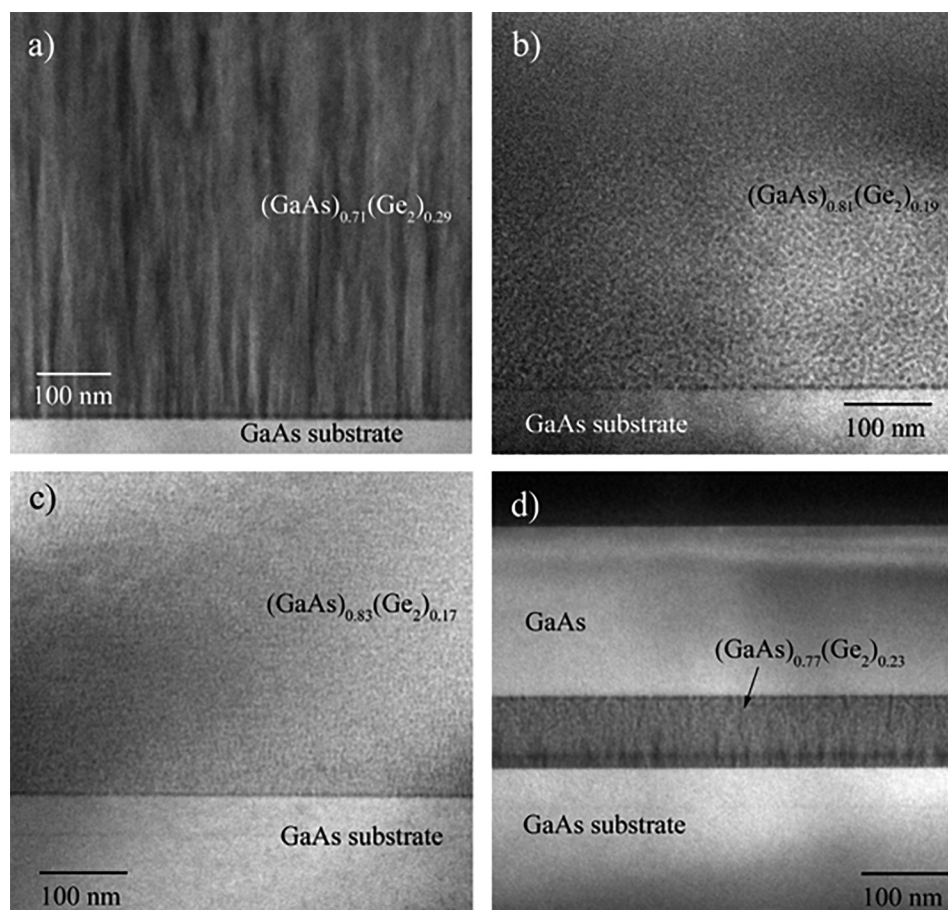


FIG. 1. (002) Darkfield XTEM images of $(\text{GaAs})_{1-x}(\text{Ge}_2)_x$ alloys. Growth temperature and system pressure are as follows: (a) 700 °C and 250 Torr. (b) 650 °C and 250 Torr. (c) 575 °C and 250 Torr. (d) GaAs – $(\text{GaAs})_{0.77}(\text{Ge}_2)_{0.23}$ – GaAs heterostructure grown at 650 °C and 250 Torr. Relatively darker regions contain more Ge compared to lighter regions.

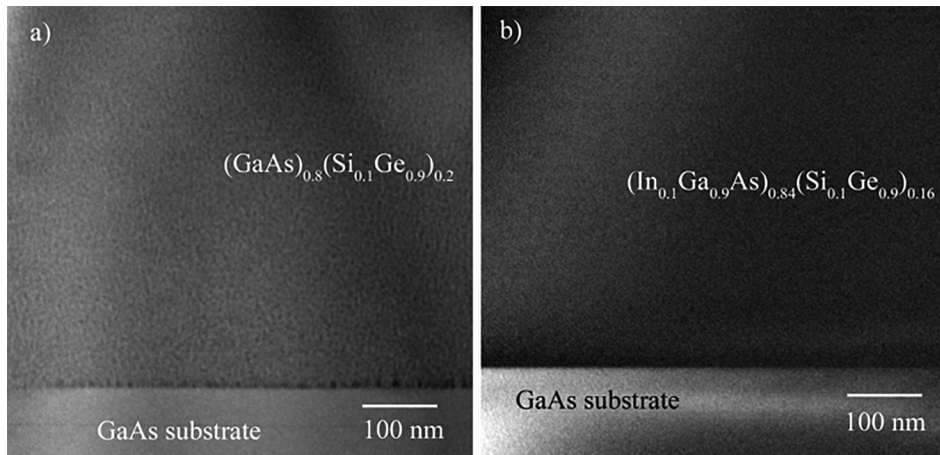


FIG. 2. (a) (002) Darkfield XTEM image of a $(\text{GaAs})_{0.8}(\text{Si}_{0.1}\text{Ge}_{0.9})_{0.2}$ alloy, grown at 650°C and 250 Torr. (b) (002) Darkfield XTEM image of an $(\text{In}_{0.1}\text{Ga}_{0.9}\text{As})_{0.84}(\text{Si}_{0.1}\text{Ge}_{0.9})_{0.16}$ alloy, grown at 575°C and 250 Torr.

The GaAs – $(\text{GaAs})_{0.77}(\text{Ge}_2)_{0.23}$ alloy – GaAs double heterostructure is shown in Fig. 1(d). APBs are normally seen in GaAs films grown on exact (001) Ge substrates.^{13,14} We obtained a high quality GaAs layer upon depositing onto the $(\text{GaAs})_{0.77}(\text{Ge}_2)_{0.23}$ alloy, with no apparent anti-phase boundaries (APBs). This suggests that the alloy film maintains predominantly a zincblende crystal lattice at the surface. The determination of the zincblende-diamond cubic order-disorder transition of the alloy was a key topic of interest in several theoretical studies that followed the original experimental study on the $(\text{GaAs})_{1-x}(\text{Ge}_2)_x$ alloys; although a consensus does not appear to have been reached on the exact location of the transition, the average composition of our alloys would be comfortably within the zincblende regime in all the studies.^{15–20} Any regions at the surface of our alloys that may be diamond cubic in nature may be sufficiently small so that rather than nucleate GaAs islands, they are overgrown by the coalescence of GaAs from the adjacent zincblende regions, preserving a single domain.

The alloys shown in Fig. 1 clearly have different morphologies from those observed by Norman *et al.*, which showed pronounced faceted phase separation.⁶ Based on their suggested growth mechanism of segregation, accumulation, and precipitation of Ge, we speculate that the growth conditions used in their samples had a much lower effect on limiting surface kinetics. The difference in surface preparation prior to depositing the alloy is one condition that may play a role in the end morphology. Our decision to conduct a 20 s N_2 ambient anneal prior to depositing the alloy stems from previous studies, indicating that As-rich surfaces are unfavorable for Ge adatom incorporation.²¹ Since the alloys are formed by codeposition of Ga, Ge, and As, an As-rich substrate surface may cause increased segregation of Ge toward the surface as Ga and As incorporate into the film.

Images of a $(\text{GaAs})_{0.8}(\text{Si}_{0.1}\text{Ge}_{0.9})_{0.2}$ alloy and an $(\text{In}_{0.1}\text{Ga}_{0.9}\text{As})_{0.84}(\text{Si}_{0.1}\text{Ge}_{0.9})_{0.16}$ alloy are shown in Figs. 2(a) and 2(b), respectively. The $(\text{In}_{0.1}\text{Ga}_{0.9}\text{As})_{0.84}(\text{Si}_{0.1}\text{Ge}_{0.9})_{0.16}$ alloy in Fig. 2(b) was grown at 575°C ; attempts at growing a sample at 650°C resulted in a defective film with a striated morphology (not shown). This contrasts with the $(\text{GaAs})_{1-x}(\text{Ge}_2)_x$ alloys, which exhibited a striated morphology only when growing at 700°C , and suggests an increased driving

force for phase separation in $(\text{In}_{0.1}\text{Ga}_{0.9}\text{As})_{0.84}(\text{Si}_{0.1}\text{Ge}_{0.9})_{0.16}$, likely due to increased strain.

Photoluminescence (PL)

Room temperature PL spectra of $(\text{GaAs})_{0.71}(\text{Ge}_2)_{0.29}$ [sample morphology in Fig. 1(a)] and $(\text{GaAs})_{0.81}(\text{Ge}_2)_{0.19}$ [sample morphology in Fig. 1(b)] are shown in Fig. 3. A $(\text{GaAs})_{0.77}(\text{Ge}_2)_{0.23}$ sample (speckle morphology; grown at 650°C) is also shown. Based on the results and those of the previous studies,^{6,7} it is clear that the sample morphology plays a key role in whether $(\text{GaAs})_{1-x}(\text{Ge}_2)_x$ exhibits room temperature PL or not. Specifically, $(\text{GaAs})_{1-x}(\text{Ge}_2)_x$ would appear to not exhibit any room temperature luminescence signal if there is a very large degree of phase separation or large compositional fluctuations. We tested several GaAs/Ge nanostructures from a previous investigation,²² which have comparable morphologies to the phase separated $(\text{GaAs})_{1-x}(\text{Ge}_2)_x$; those structures also did not exhibit any room temperature PL, consistent with the idea that the luminescence signal comes from atomically mixed regions of

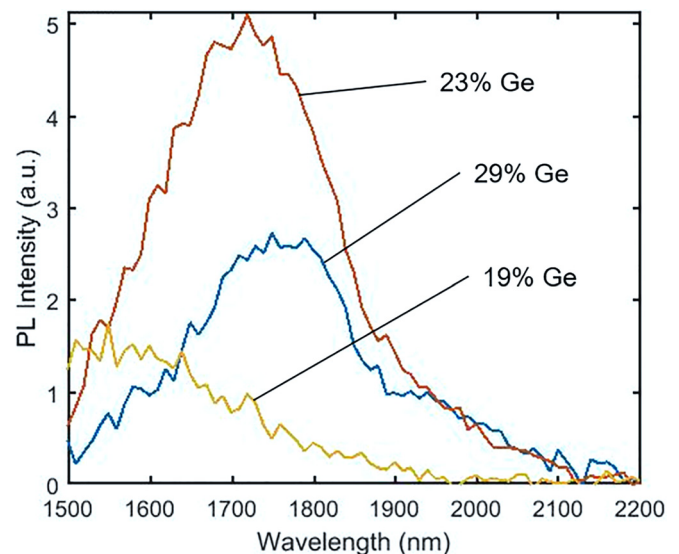


FIG. 3. Room temperature photoluminescence spectra of $(\text{GaAs})_{0.81}(\text{Ge}_2)_{0.19}$, $(\text{GaAs})_{0.77}(\text{Ge}_2)_{0.23}$, and $(\text{GaAs})_{0.71}(\text{Ge}_2)_{0.29}$ alloys. Luminescence peaks at approximately 1550 nm (0.8 eV), 1720 nm (0.72 eV), and 1760 nm (0.7 eV), respectively.

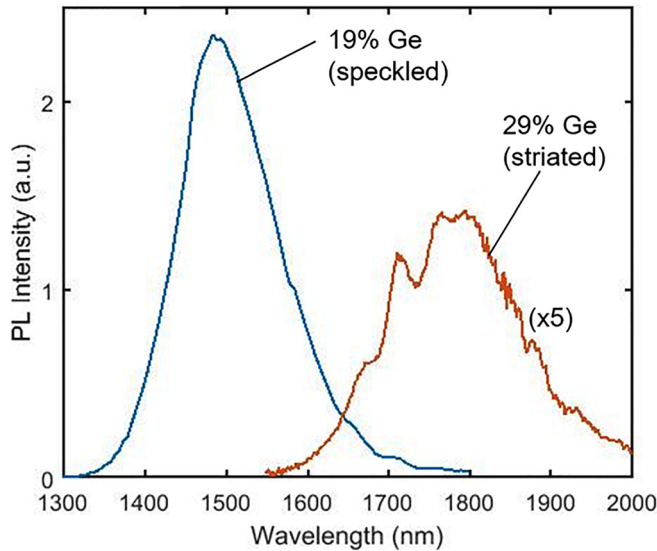


FIG. 4. 77 K photoluminescence spectrum of the striated $(\text{GaAs})_{0.71}(\text{Ge}_2)_{0.29}$, with multiple luminescence peaks resolved. These peaks likely correspond to different striated regions in the structure. The 77 K photoluminescence spectrum of the speckled $(\text{GaAs})_{0.81}(\text{Ge}_2)_{0.19}$ is also shown.

$(\text{GaAs})_{1-x}(\text{Ge}_2)_x$. Figure 4 shows the photoluminescence spectrum of $(\text{GaAs})_{0.71}(\text{Ge}_2)_{0.29}$ and $(\text{GaAs})_{0.81}(\text{Ge}_2)_{0.19}$ measured at 77 K. The effect of the different degrees of composition modulation is apparent—multiple peaks are resolved in the $(\text{GaAs})_{0.71}(\text{Ge}_2)_{0.29}$ sample, likely corresponding to different striation compositions. In contrast, the speckled $(\text{GaAs})_{0.81}(\text{Ge}_2)_{0.19}$ sample still exhibits one peak.

Room temperature PL spectra of several samples with a Ge composition less than 20% are shown in Fig. 5. All samples had a peak luminescence at 1550 nm (0.8 eV); the luminescence intensity decreased as the composition of Ge decreased. These data are not consistent with the previous studies, which estimate that $(\text{GaAs})_{1-x}(\text{Ge}_2)_x$ alloys with 19%, 17%, 12%, and 6% Ge compositions have approximate bandgaps of 0.85 eV, 0.9 eV, 1.04 eV, and 1.22 eV,

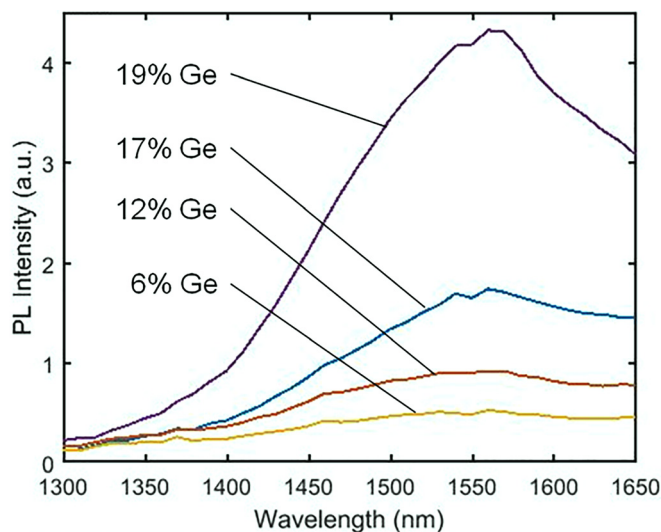


FIG. 5. Room temperature photoluminescence spectra of $(\text{GaAs})_{1-x}(\text{Ge}_2)_x$ alloy samples with Ge compositions less than 20%. Luminescence peaks of all samples at approximately 1550 nm. The luminescence intensity decreases with the decreasing Ge composition.

respectively.^{5,16,17} It is likely that bandgap narrowing occurs as a result of the composition fluctuations in the samples; various groups have observed this phenomenon in III-V ternary and quaternary alloys that exhibit composition fluctuations.^{8,23–25} Fluctuations result in regions with higher Ge compositions than the alloy average and thus would have smaller bandgaps. Electron-hole pairs generated in nearby regions would relax to these lower energy regions before recombining, resulting in luminescence peaks at longer wavelengths than expected. However, the emission wavelength remains the same since recombination occurs in similar Ge-rich regions. The intensity increases with the Ge concentration because there are more light-emitting Ge-dominate areas.

The TEM results suggest that these composition fluctuations are very fine spatially, and our PL observations are consistent with such a description. Moreover, as we have previously published,²² the $(\text{GaAs})_{1-x}(\text{Ge}_2)_x$ alloys have high electron mobility, generally $>1000 \text{ cm}^2/\text{V s}$ with doping in the range of 10^{17} cm^{-3} . Thus, the electron wavelength must be much greater than the composition fluctuations; otherwise, there would be increased scattering and low mobility.

The room temperature photoluminescence spectrum of the $(\text{GaAs})_{0.8}(\text{Si}_{0.1}\text{Ge}_{0.9})_{0.2}$ alloy is shown in Fig. 6. The spectrum of the $(\text{GaAs})_{0.81}(\text{Ge}_2)_{0.19}$ alloy is also shown for comparison. The $(\text{GaAs})_{0.8}(\text{Si}_{0.1}\text{Ge}_{0.9})_{0.2}$ peak is slightly blueshifted relative to the $(\text{GaAs})_{0.81}(\text{Ge}_2)_{0.19}$ peak. Si has a larger bandgap than Ge; therefore, we can expect this blueshift to be due to the presence of Si increasing in the bandgap of the alloy structure that emits light. This result suggests the possibility of engineering the range of low bandgaps above 0.8 eV using III-IV-V alloys as an alternative to finding the growth conditions needed to fully inhibit composition fluctuations in $(\text{GaAs})_{1-x}(\text{Ge}_2)_x$, which thus far remains elusive. It also suggests that smaller bandgaps could be created at smaller lattice constants using similar principles in alloy systems containing some or all of the elements from InGaSiGeAsPSb. It is likely that III-IV-V alloys will reveal a variety of interesting optical, electronic, and thermoelectric properties.

CONCLUSION

III-IV-V alloys were successfully grown by MOCVD; the morphologies of these alloys were significantly different from those observed in past studies. Specifically, these alloys exhibit composition fluctuations similar to those seen in many ternary and quaternary III-V alloys rather than pronounced phase separation. Room temperature photoluminescence was observed in the alloys, a result that has potentially significant implications for small bandgap optical applications lattice-matched to GaAs. The luminescence peaks of $(\text{GaAs})_{1-x}(\text{Ge}_2)_x$ alloys were not consistent with the bandgap-composition correlation in past studies—the highest energy transition observed was 0.8 eV despite several alloys investigated with compositions corresponding to larger bandgaps. The aforementioned composition fluctuations are likely responsible for the bandgap narrowing. We have apparently created what is effectively a Ge-like solid

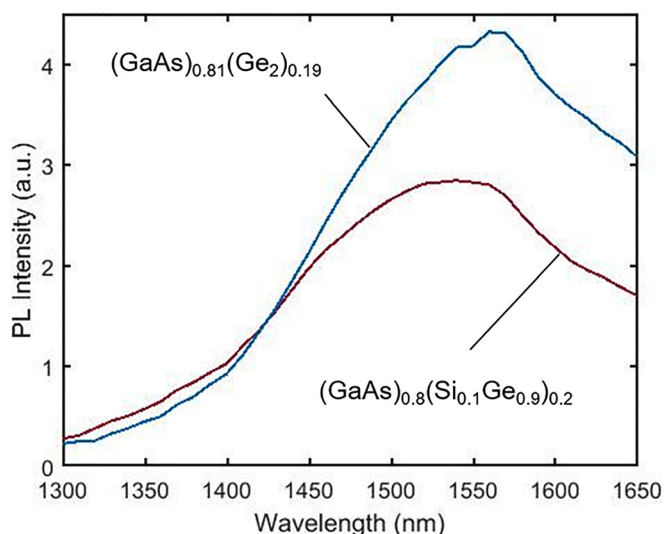


FIG. 6. Comparison of the photoluminescence spectra at room temperature for $(\text{GaAs})_{0.8}(\text{Si}_{0.1}\text{Ge}_{0.9})_{0.2}$ and $(\text{GaAs})_{0.8}(\text{Ge}_2)_{0.19}$. The addition of Si causes a blueshift in the peak luminescence.

penetrating a GaAs lattice, resulting in optical properties similar to those of Ge but with a direct-bandgap nature. The features that result in these properties are at a very small scale, also allowing high electron mobility as demonstrated in our previous publication.

By further alloying $(\text{GaAs})_{1-x}(\text{Ge}_2)_x$ with Si, we observe a blueshift in the energy transition. Thus, it may be possible to engineer a range of small bandgaps through alloying of additional elements. III-IV-V alloys are likely to demonstrate interesting electrical, optical, and thermoelectric properties on previously unattainable lattice constants.

ACKNOWLEDGMENTS

This work was supported under a research grant from the Singapore-MIT Alliance for the Research and Technology Low Energy Electronic Systems Program, a research program funded by the National Research Foundation of Singapore. This work was also supported by the Energy Frontier Research Center funded by the U.S. Department of Energy, Office of Science, Office of Basic

Energy Sciences under Award No. DESC0001088 and made use of the shared facilities supported by the eni-MIT Solar Frontiers Center. This work made use of the MRSEC Shared Experimental Facilities at MIT, supported by the National Science Foundation under Award DMR-14-19807.

- ¹D. J. Friedman, J. F. Geisz, S. R. Kurtz, and J. M. Olson, *J. Cryst. Growth* **195**, 409 (1998).
- ²T. W. Kim, T. J. Garrod, K. Kim, J. J. Lee, S. D. LaLumondiere, Y. Sin, W. T. Lotshaw, S. C. Moss, T. F. Kuech, R. Tataavarti, and L. J. Mawst, *Appl. Phys. Lett.* **100**, 121120 (2012).
- ³J. F. Geisz, S. Kurtz, M. W. Wanlass, J. S. Ward, A. Duda, D. J. Friedman, J. M. Olson, W. E. McMahon, T. E. Moriarty, and J. T. Kiehl, *Appl. Phys. Lett.* **91**, 023502 (2007).
- ⁴S. A. Barnett, M. A. Ray, A. Lastras, B. Kramer, J. E. Greene, P. M. Raccach, and L. L. Abels, *Electron. Lett.* **18**, 891 (1982).
- ⁵K. E. Newman, A. Lastras-Martinez, B. Kramer, S. A. Barnett, M. A. Ray, J. D. Dow, J. E. Greene, and P. M. Raccach, *Phys. Rev. Lett.* **50**, 1466 (1983).
- ⁶A. G. Norman, J. M. Olson, J. F. Geisz, H. R. Moutinho, A. Mason, M. M. Al-Jassim, and S. M. Vernon, *Appl. Phys. Lett.* **74**, 1382 (1999).
- ⁷S. M. Vernon, M. M. Sanfacon, and R. K. Ahrenkiel, *J. Electron. Mater.* **23**, 147 (1994).
- ⁸K. Mukherjee, D. A. Beaton, T. Christian, E. J. Jones, K. Alberi, A. Mascarenhas, M. T. Bulsara, and E. A. Fitzgerald, *J. Appl. Phys.* **113**, 183518 (2013).
- ⁹G. B. Stringfellow, *J. Cryst. Growth* **65**, 454 (1983).
- ¹⁰S. Mahajan, *Mater. Sci. Eng., B* **30**, 187 (1995).
- ¹¹S. N. G. Chu, S. Nakahara, K. E. Strege, and W. D. Johnston, Jr., *J. Appl. Phys.* **57**, 4610 (1985).
- ¹²A. Diéguez, F. Peiró, A. Cornet, J. R. Morante, F. Alsina, and J. Pascual, *J. Appl. Phys.* **80**, 3798 (1996).
- ¹³S. M. Ting and E. A. Fitzgerald, *J. Appl. Phys.* **87**, 2618 (2000).
- ¹⁴H. Kroemer, *J. Cryst. Growth* **81**, 193 (1987).
- ¹⁵J. E. Greene, *J. Vac. Sci. Technol. B* **1**, 229 (1983).
- ¹⁶B. Koiller, M. A. Davidovich, and R. Osório, *Solid State Commun.* **55**, 861 (1985).
- ¹⁷K. E. Newman and J. D. Dow, *Phys. Rev. B* **27**, 7495 (1983).
- ¹⁸K. E. Newman, J. D. Dow, B. A. Bunker, L. L. Abels, P. M. Raccach, S. Ugur, D. Z. Xue, and A. Kobayashi, *Phys. Rev. B* **39**, 657 (1989).
- ¹⁹G. Giorgi, M. V. Schilfgaarde, A. Korkin, and K. Yamashita, *Nanoscale Res. Lett.* **5**, 469 (2010).
- ²⁰B.-L. Gu, J. Ni, and J.-L. Zhu, *Phys. Rev. B* **45**, 4071 (1992).
- ²¹Y. Bai, K. E. Lee, C. Cheng, M. L. Lee, and E. A. Fitzgerald, *J. Appl. Phys.* **104**, 084518 (2008).
- ²²R. Jia, L. Zeng, G. Chen, and E. A. Fitzgerald, *Appl. Phys. Lett.* **110**, 222105 (2017).
- ²³A. G. Norman, T.-Y. Seong, I. T. Ferguson, G. R. Booker, and B. A. Joyce, *Semicond. Sci. Technol.* **8**, S9 (1993).
- ²⁴S. W. Jun, T. Seong, J. H. Lee, and B. Lee, *Appl. Phys. Lett.* **68**, 3443 (1996).
- ²⁵K. A. Mäder and A. Zunger, *Phys. Rev. B* **51**, 10462 (1995).